PHYSICAL REVIEW A VOLUME 18, NUMBER 6 DECEMBER 1978

Fine-structure intervals and polarizabilities of highly excited d states of K

T. F. Gallagher and W. E. Cooke
Molecular Physics Laboratory, SRI International, Menlo Park, California 94025
(Received 17 July 1978)

The fine-structure (fs) intervals and polarizabilities of K $n = 15$–20 d states have been measured using a radio-frequency resonance-selective field-ionization approach. Although there is no apparent difference in the field-ionization characteristics of the $d_{3/2}$ and $d_{5/2}$ states when excited in zero electric field, we are able to observe the resonances by using a small dc electric field and time-resolved detection. The fine-structure intervals of the K d states for $n \sim 20$ are inverted. Specifically, the observed fs intervals (in MHz) are: $15d$, $-375.33(40)$; $16d$, $-306.25(15)$; $18d$, $-211.68(20)$; $20d$, $-152.42(45)$. The observed tensor polarizabilities [in MHz/(V/cm)^2] are: $15d$, $-0.0208(9)$; $16d$, $-0.0315(8)$; $18d$, $-0.0681(18)$; $20d$, $-0.1349(40)$.

I. INTRODUCTION

For decades the fine structure (fs) of alkali atoms has been a subject of continuous interest. Recently there has been a renewed interest since the tunable dye laser has made it possible to carry out systematic, high-resolution studies of alkali fs as a function of the principal quantum number n and l. Here we shall restrict our attention to the variation of d-state fs with n. Recently, Cooke *et al.*[1] have shown that the fs of the Li d states are hydrogenic to within 1% from $n = 7$–11. Fabre *et al.*[2] have shown that the fine structure of Na d states is inverted (the $J = \frac{5}{2}$ state lies above the $J = \frac{5}{2}$ state), that the magnitude of the interval is about equal to that of hydrogen, and that the intervals are well represented by $A/(n^*)^3 + B/(n^*)^5$, where n^* is the effective quantum number. In Rb, Kato and Stoicheff[3] and Harvey and Stoicheff[4] have recently shown that, although the fs intervals are much larger than H, the intervals can again be represented by $A/(n^*)^3 + B/(n^*)^5$ for all values of n^*. For Na, $A < 0$ and $B > 0$, and for Rb $A > 0$ and $B < 0$. In the case of Rb the magnitude of B is large enough that the fs of the Rb $4d$ state is inverted. As we shall see, the behavior of the K fs affords a curious contrast.

Along with the recent experimental progress has come significant theoretical progress. Notable recent successes are the calculations of inverted Na d fs by Holmgren *et al.*,[5] Luc-Koenig,[6] and Foley and Sternheimer,[7] and the calculation of the Rb $4d$ fs by Lee *et al.*[8]

The polarizabilities of excited atoms are of interest because, much as for a ground-state atom, the polarizability of an excited atom is the parameter that characterizes how the atom interacts with a weak external electric field, whether it be a macroscopic field or the microscopic field from another atom or molecule. Thus the polarizabilities play a role in collisions and field ionization of Rydberg atoms.

Here we report the measurement of a series of fs intervals and polarizabilities of K d states using a radio frequency (rf) resonance technique. We have used a selective field ionization method related to one we have used previously for Na.[9] However, a more subtle approach was required due to dramatic differences in the field ionization behavior of Na and K.

II. ENERGY LEVELS AND HAMILTONIAN

Before considering the details such as the fs of K, it is worth considering the gross features of the K spectrum. To this end the K energy levels for $n \sim 18$ are shown in Fig. 1, which shows the energy levels as a function of electric field (on this scale the fs intervals are too small to resolve). Note in particular that the energy of the $18d$ state is depressed as the field is increased, due mainly to the proximity of the $18f$ level.

The Hamiltonian for the energy levels of the K atom in a weak electric field E can be written[10]

$$\mathcal{H} = \mathcal{H}_{\text{Coul}} + \mathcal{H}_{fs} - \frac{\alpha_0 E^2}{2} - \frac{\alpha_2 E^2}{2}\left(\frac{3m_j^2 - J(J+1)}{J(2J-1)}\right). \tag{1}$$

$\mathcal{H}_{\text{Coul}}$ represents the Coulomb interaction of the valence electron with the ionic core. The energy W of each principal series of l is given (in atomic units) by

$$W = -1/2n^{*2}, \tag{2}$$

where $n^* = n - \delta_l$ and δ_l is the quantum defect of the l state. For K the quantum defects of the s, p, d, and f states are 2.15, 1.70, 0.27, and 0.007,

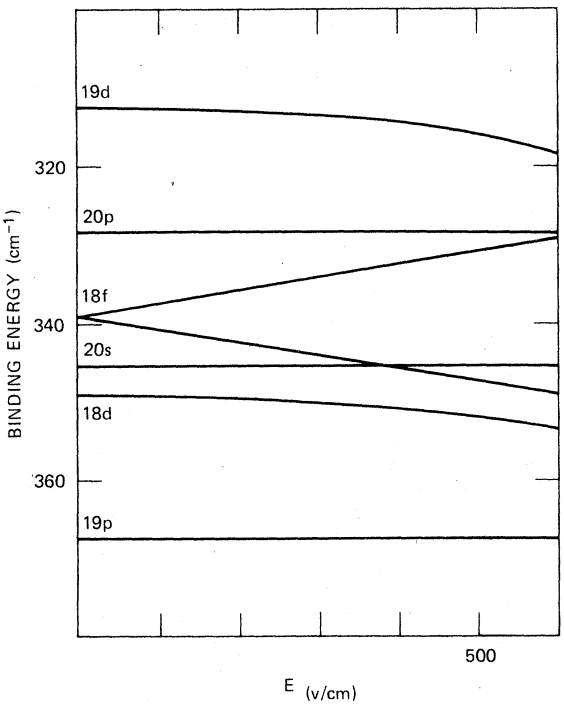

FIG. 1. K energy levels near $n = 18$ as a function of electric field. In the field regime shown the higher l states exhibit a linear Stark effect and fall between the two lines diverging from $18f\cdots$. In these fields the Stark effect of the s, p, and d states is quadratic and only appreciable for d states.

respectively. As a result of the different quantum defects, l states of the same n are not degenerate but have different energies as shown by Fig. 1. $\mathcal{H}_{fs}$ represents the spin-orbit coupling which is of the form $\vec{L}\cdot\vec{S}$. The $\alpha_0 E^2$ and $\alpha_2 E^2$ terms are the leading terms in the perturbation expansion for the Stark effect (in even powers of E). Such an expansion may be used to express the energy of a state only for fields weak enough that the Stark shift is less than the fs interval, a condition that is met in our experiments. At fields somewhat below where the perturbation expansion becomes invalid, the higher-order E^4 and E^6 terms in the Stark effect begin to appear due to the uncoupling of $\vec{L}$ and $\vec{S}$. α_0 and α_2 are, respectively, the scalar and tensor polarizabilities which characterize the second-order Stark shift. α_0 describes the common displacement of all the m_j states of a given J, and α_2 determines the splitting of the m_j levels. In Eq. (1) we have neglected the effect of hyperfine structure which is negligible in our experiments.[11]

Khadjavi *et al.*[6] have derived general expressions for the polarizabilities α_0 and α_2 which depend on angular factors in the form of 6-j symbols and the energy differences and radial matrix elements between states coupled by the electric field. Their results can be simplified in the event that the fine-structure splittings are small compared to the Δl energy separations; for then, in addition, the radial matrix elements for the two fine-structure states of the same l are the same. In this case the polarizabilities $\alpha_0(J)$ and $\alpha_2(J)$ of the nd_j states (in atomic units) can be written

$$\alpha_0(\tfrac{3}{2}) = \alpha_0(\tfrac{5}{2}) = -\tfrac{4}{15}P - \tfrac{2}{5}F\,, \tag{3a}$$

$$\tfrac{10}{7}\alpha_2(\tfrac{3}{2}) = \alpha_2(\tfrac{5}{2}) = \tfrac{4}{15}P + \tfrac{4}{35}F\,. \tag{3b}$$

Here

$$P = \sum_{n'} \left| \int R(nd)R(n'p)r\,dr \right|^2 \Big/ (E_{n_d} - E_{n'_p})\,, \tag{4}$$

$$F = \sum_{n'} \left| \int R(nd)R(n'f)r\,dr \right|^2 \Big/ (E_{n_d} - E_{n'_f})\,,$$

where $R(nl)$ is the radial wave function and E_{nl} the energy of the n_l state. Note that the scalar polarizabilities of both J levels are equal and that the tensor polarizabilities are related by the factor of $\frac{10}{7}$. To simplify the notation let us rewrite the polarizabilities

$$\alpha_0 = \alpha_0(\tfrac{5}{2}) = \alpha_0(\tfrac{3}{2}), \quad \alpha_2 = \alpha_2(\tfrac{5}{2}) = \tfrac{10}{7}\alpha_2(\tfrac{3}{2})\,. \tag{5}$$

It is worth noting that the above-mentioned simplification occurs for both Na and K, where the fs intervals are small compared to the Δl separations, but not for Cs. The validity of this simplification has been verified experimentally by Harvey *et al.*[12] and Hawkins *et al.*,[13] who have shown that for Na d states that $\alpha_0(\frac{5}{2}) = \alpha_0(\frac{3}{2})$ to within 1% and that $\alpha_2(\frac{5}{2}) = \frac{10}{7}\alpha_2(\frac{3}{2})$ to within 3%.

We may estimate the signs of α_0 and α_2 using Eqs. (3) and (4). In the F and P sums of Eq. (4) the terms for which n' is nearest n dominate both because the energy dominators are the smallest and because the dipole matrix elements are the largest. Thus for the $18d$ state we would expect the F sum to be large and negative due to the presence of the $18f$ state just above the $18d$ state as shown in Fig. 1. Since the $18d$ state is roughly midway between the $19p$ and $20p$ states we would expect their effects to cancel, resulting in P being small compared to F. Thus α_0 and α_2 would be mainly determined by F, with the result that $\alpha_0 > 0$ and $\alpha_2 < 0$. Note that $\alpha_0 > 0$ is in agreement with the downward energy shift of the $18d$ state in an electric field as shown in Fig. 1. As we shall see, the sign of α_2 is important in determining the sign of S_d, the fs interval.

In Fig. 2 we show energy level diagram of the K $18d$ state in the low electric field used in these

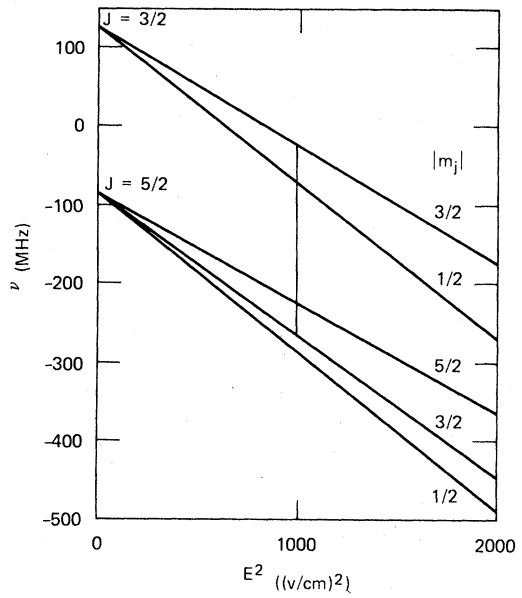

FIG. 2. Energy level diagram for the K d fs states in weak electric fields. The line indicates the transition we observe.

experiments. The diagram is drawn for $S_d < 0$, $\alpha_0 > 0$, and $\alpha_2 < 0$ (which we shall see to be true). The solid line indicates the transition we observe in the experiments, the $\Delta m_j = 0$ transition $d_{5/2}|m_j| = \frac{3}{2} \rightarrow d_{3/2}|m_j| = \frac{3}{2}$. From Eq. (1) we can calculate the frequency of the transition to be

$$\nu = \left| S_d + \tfrac{9}{20}\alpha_2 E^2 \right| . \tag{6}$$

The absolute value sign is to avoid the possibility of a negative frequency. Note in particular that if α_2 and S_d are of the same sign that ν increases with E^2.

III. EXPERIMENTAL METHOD

In Fig. 3 we illustrate the basic idea of the experiment for the K 18d state. We use two pulsed dye lasers to excite K atoms in an atomic beam to the $18d_{5/2}$ state via the transitions $4p_{1/2} \rightarrow 4p_{3/2}$, $4p_{3/2} \rightarrow 18d_{5/2}$. Immediately following the laser excitation we use an rf field to induce the $18d_{5/2} \rightarrow 18d_{3/2}$ transition. About 0.7 μsec after the laser excitation we field ionize the atoms in the 18d state in such a way that we selectively detect those in the $18d_{3/2}$ state. Thus when the frequency of the rf field is not tuned to the $18d_{5/2}$–$18d_{3/2}$ resonance there is no signal, but as the frequency is swept through the resonance there is a dramatic increase in the signal as shown in Fig. 4.

The method is analogous to the molecular-beam-resonance approach, and as a consequence the

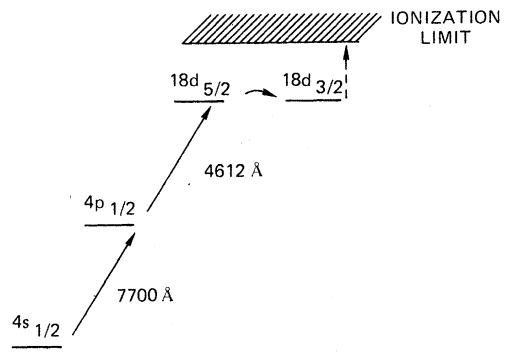

FIG. 3. Relevant energy levels for the experiment on the K 18d state. The straight arrows pointing up indicate the two-step laser pumping of the $18d_{5/2}$ state. The curved arrow indicates the rf-induced fs transition and the dotted arrow indicates the selective ionization of the $18d_{3/2}$ state.

selective population and detection are crucial to the experiment. Selective population is straightforward. We can take advantage of the much larger $\Delta J = 1$ than $\Delta J = 0$ dipole matrix elements to populate either the $18d_{5/2}$ or $18d_{3/2}$ state by using the $4p_{3/2}$ or $4p_{1/2}$ state, respectively, as the immediate state in the laser pumping. In addition, if we apply a weak (~10–100 V/cm) dc electric field and polarize the laser so that $\vec{E}_{\text{laser}} \| \vec{E}_{\text{dc}}$ we can take advantage of the $\Delta m_j = 0$ selection rules to populate only $|m_j| = \frac{1}{2}$ or $\frac{3}{2}$ states of the $18d_{5/2}$ state or only the $|m_j| = \frac{1}{2}$ state of the $18d_{3/2}$ state.

The selective detection of the excited K d states poses a more subtle problem. It is useful first to examine the ionization behavior of the K 18d state that is typical of all the K d states. In Fig. 5 we show a plot of total (time-integrated) ionization current versus the peak field attained in the ionization pulse for the $18d_{5/2}$ state (zero dc field). There are three ionization thresholds, two nearly overlapping at 3.63 and 3.68 kV/cm, and the third at 3.98 kV/cm is clearly resolved. The analogous trace for the $18d_{3/2}$ state is identical, so at first glance it seems impossible to contemplate doing a resonance experiment using field ionization as a state-selective detector. We should note that the similarity of the field ionization behavior of the two K d fs states is radically different from what we observed in Na.[14] This difference arises in the passage from low to high field when the field from the ionizing pulse is applied. We shall not discuss the details of the field ionization of K here as they are discussed in detail elsewhere.[15]

The method used to do the resonance experiments becomes apparent when the thresholds are identified, to the extent possible. To identify at

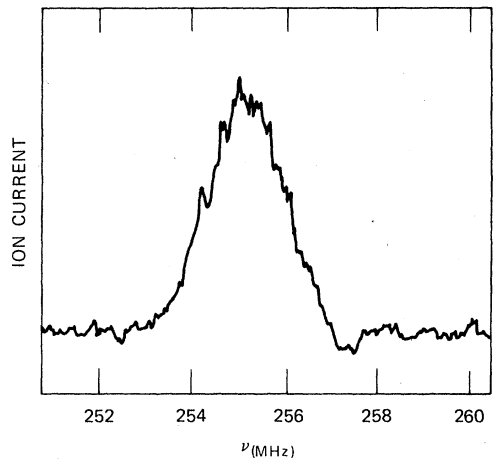

FIG. 4. $18d_{5/2} \rightarrow 18d_{3/2}$ resonance observed in dc field of 35.6 V/cm on a sweep of decreasing frequency.

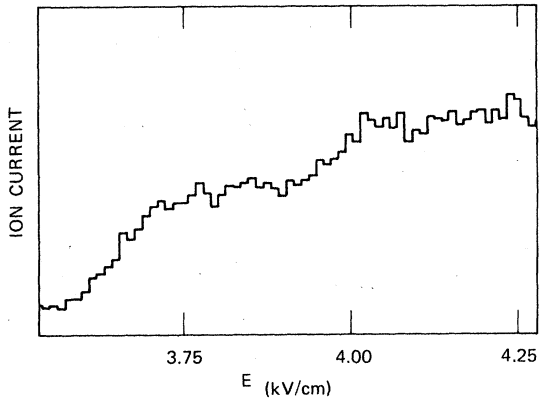

FIG. 5. Field ionization thresholds observed for the $18d_{5/2}$ state. There are two unresolved thresholds at 3.63 and 3.68 kV/cm and one clearly resolved threshold at 3.98 kV/cm.

least partially the thresholds of Fig. 5, we applied a dc field of 20 V/cm and polarized the second laser so that $E_{\text{laser}} \| E_{\text{dc}}$. Then the threshold at 141 V disappeared for both the $d_{3/2}$ and $d_{5/2}$ states. Therefore the $\Delta m_j = 0$ selection rule implies that these thresholds must be due to only the $|m_j| = \frac{3}{2}$ and $\frac{5}{2}$ states for the $d_{3/2}$ and $d_{5/2}$ states, respectively. Thus we can construct Table I, which gives the possible $|m_j|$ states that can contribute to each threshold. The parentheses around entries indicate that we doubt that there is any contribution from these states but that the evidence is not conclusive. However, this uncertainty in no way affects the resonance experiments described here.

From Table I it is clear why we chose to study the $\Delta m_j = 0$ $d_{5/2} \rightarrow d_{3/2} |m_j| = \frac{3}{2}$ transition. All atoms in the $18d_{5/2} |m_j| = \frac{3}{2}$ state ionize at the 3.63–3.68 kV/cm threshold, none of them ionize at the 3.98 kV/cm threshold. However most of the atoms in the $18d_{3/2} |m_j| = \frac{3}{2}$ state ionize at the 3.98 kV/cm threshold. Thus there is a clear difference in the ionization behavior of the $18d_{5/2} |m_j| = \frac{3}{2}$ and $18d_{3/2} |m_j| = \frac{3}{2}$ states which, in principle, makes this transition observable. Note that the other $\Delta m_j = 0$ transition $18d_{5/2} \rightarrow 18d_{3/2} |m_j| = \frac{1}{2}$ is not observable.

TABLE I. Threshold fields for ionization of potassium $18d$ states.

J	3.63–3.68 kV/cm $\lvert m_j \rvert$	3.98 kV/cm $\lvert m_j \rvert$
$\frac{3}{2}$	$\frac{1}{2}$, $(\frac{3}{2})$	$\frac{3}{2}$
$\frac{5}{2}$	$\frac{1}{2}$, $\frac{3}{2}$, $(\frac{5}{2})$	$\frac{5}{2}$

By combining the selective excitation and detection we are able to do the resonance experiment. We populate the $18d_{5/2}$ state with the second laser polarized so that $\vec{E}_{\text{laser}} \| \vec{E}_{\text{dc}}$, ensuring that we populate only the $|m_j| = \frac{1}{2}$ and $\frac{3}{2}$ states. Using an rf electric field such that $\vec{E}_{\text{rf}} \| \vec{E}_{\text{dc}}$ we can induce the $\Delta m_j = 0$ transition $18d_{5/2} |m_j| = \frac{3}{2} \rightarrow 18d_{3/2} |m_j| = \frac{3}{2}$ populating the $18d_{3/2} |m_j| = \frac{3}{2}$ state. We detect this population using time-resolved detection of the field ionization. We set the amplitude of the field ionization pulse to 4.03 kV/cm, which is high enough to ionize all atoms in the $18d$ state. Since the ionization pulse is not a sharp step but has a finite rise time of about 300 nsec, atoms ionized at the 3.98 kV/cm threshold are detected ~70 nsec after those which are ionized at the 3.63–3.68 kV/cm threshold. Thus atoms in the initially populated $18d_{5/2} |m_j| = \frac{1}{2}, \frac{3}{2}$ states are ionized first. Those atoms which have undergone a transition to the $18d_{3/2} |m_j| = \frac{3}{2}$ state are not ionized until later when the field reaches 3.98 kV/cm. Examples of the time-resolved ion signals are shown in Fig. 6. Figure 6(a) shows the ion pulse from the threshold at 3.63–3.68 kV/cm. We have arbitrarily labeled its arrival time to be $t = 0$. In Fig. 6(b) we show the ion signal when the rf field is tuned to resonance. The ion signal from the 3.98 kV/cm threshold is clearly apparent at $t = 70$ nsec. To do the experiments we simply set the boxcar averager gate, which is 60 nsec wide, at $t = 70$ nsec in Fig. 6. Thus there is normally no signal, but on resonance there is

an easily observed increase in the ion current. It is worth noting that the total (time-integrated) ion current is the same on or off resonance, so the time-resolved detection is essential.

In these experiments we used the electric resonance method first used by Hughes.[16] In the presence of a weak electric field it is possible to drive the $d_{5/2} \rightarrow d_{3/2}$ transition with an rf electric field because the dc electric field admixes a small amount of states of the opposite parity. Due to the large electric dipole matrix elements at $n = 18$ rf electrics fields ~1 V/cm are required when dc fields of ~20 V/cm are used. At frequencies of 200–400 MHz it is considerably easier to generate electric fields of 1 V/cm than the magnetic fields of 1 G that would be required to drive the magnetic dipole transitions. Thus the motivation for using the electric resonance technique was its ease. To generate the rf we used a Hewlett-Packard 3200B signal generator and a General Radio 1208B signal generator. The frequency was monitored with a Hewlett-Packard 5245L counter with a 5253B converter, leading to an accuracy of better than ±0.1 MHz.

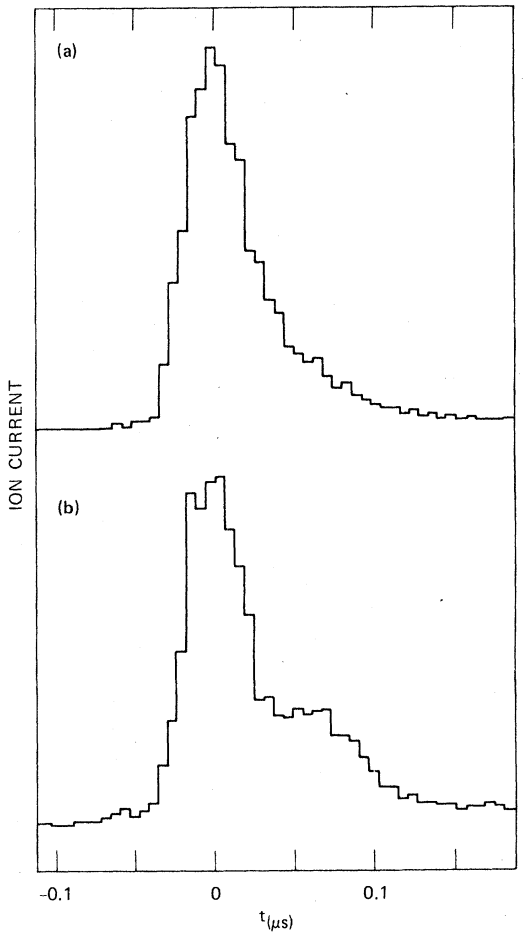

FIG. 6. Time-resolved ion signals from the $18d$ state with an ionizing field of 4.03 kV/cm and 27 V/cm dc bias field. (a) Signal from the $18d_{3/2}$ state excited with $\vec{E}_{\text{laser}} \| \vec{E}_{\text{dc}}$. (b) Signal with rf tuned to the $18d_{5/2} \rightarrow 18d_{3/2}$ resonance. The second ionization pulse at $t = 70$ nsec is due to the atoms which have made the transition to the $18d_{3/2} |m_j| = \frac{3}{2}$ states.

The laser atomic beam apparatus is of conventional design,[17,18] and only the interaction region is of particular interest. As shown in Fig. 7 the atomic beam is crossed by the laser beams between plate b and grid c, which are 1.12 cm apart. A positive high voltage pulse is applied to plate b 0.7 μsec after the laser pulse. The rf is continuously introduced by a 50-Ω cable terminated with a 50-Ω resistor as shown in Fig. 7. To minimize the effect of the high voltage (−2000 V) on the front of the electron multiplier the grounded grid d was inserted. To determine the magnitude of the field introduced by the multiplier we checked the frequencies of the observed transitions with dc fields of +40 and −40 V, and from the shift determined that the leakage field from the multiplier was 0.140 V/cm. This was used to correct the measured dc fields.

For each nd state resonances were observed for several values of dc field as shown in Fig. 8. Each point of Fig. 8 corresponds to a sweep of increasing and decreasing frequency to cancel the offsets (~0.2 MHz) produced by the time constant of the boxcar averager.

IV. RESULTS

As shown in Fig. 8, the resonance frequency increases with E^2 thus S_d and α_2 have the same sign. Since an inspection of the energy level dia-

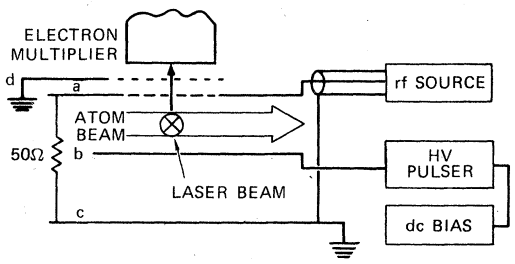

FIG. 7. Interaction region. The atomic beam is crossed by the laser beams (shown going into the paper) between grid a and plate b. The high-voltage ionizing pulse is applied to plate b that ionizes the atoms and accelerates the ions through the grid and into the electron multiplier. The rf is introduced by a 50-Ω coaxial cable that is terminated by a 50-Ω resistor between grid a and grounded plate c. Grid d serves to shield the leakage field from the electron multiplier.

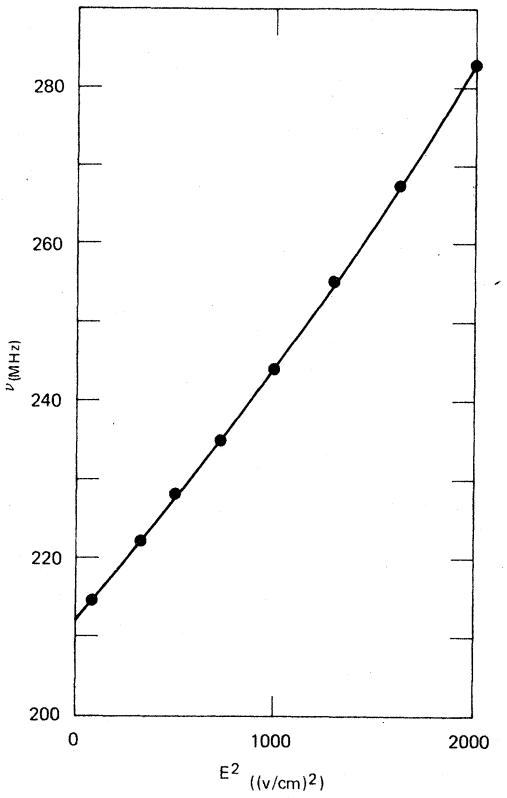

FIG. 8. Plot of the observed frequency vs E^2 for $18d$, as well as the fit to the data using Eq. (7).

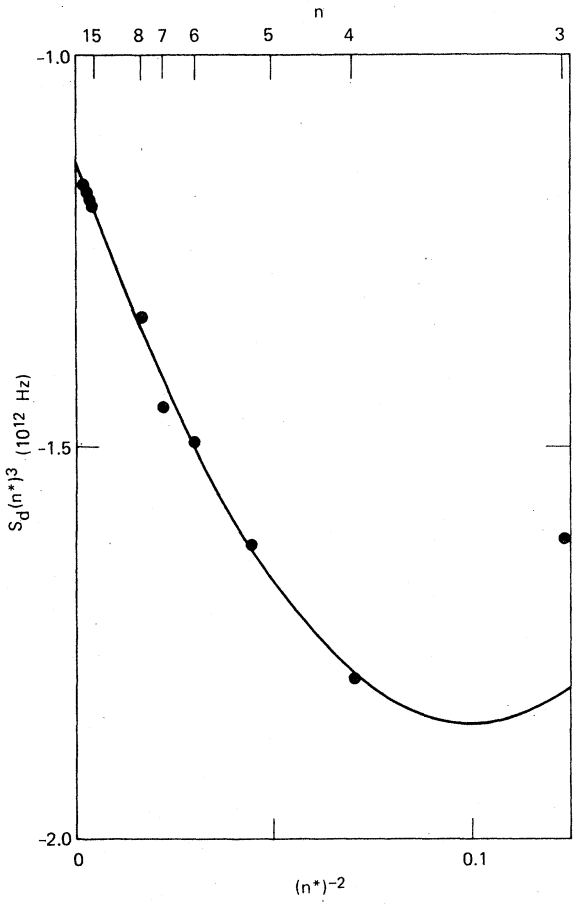

FIG. 9. Plot of $S_d\,(n^*)^3$ vs $(n^*)^{-2}$. The curve is fit to the data using Eq. (8). The data for $n \leq 8$ are from Ref. 23.

gram of Fig. 1 and Eqs. (3) and (4) implies that $\alpha_2 < 0$ it is clear that $S_d < 0$ and that the fs is inverted. Extrapolating from the values from lower n this is hardly unexpected.

In Fig. 8 it is also apparent that the frequency variation is not linear in E^2 but at least quadratic. Thus we extended Eq. (6) and fit the data to the form

$$D = \left| S_d + \tfrac{9}{20}\alpha_2 E^2 + \gamma E^4 \right|, \qquad (7)$$

where γ is related to the hyperpolarizability.[19] The results are given in Table II along with the values of α_2 and α_0 for $n \leq 18$ calculated using the Bates-Damgaard method.[20,21] The very close agreement between the measured and calculated values of α_2 gives us confidence in the calculated values of α_0. Unfortunately we were unable to calculate values for the $n = 20$ radial matrix elements; the numerical problem was simply beyond the capabilities of our computer.

The fs intervals of the alkali atoms can be fit to a power series in odd inverse powers of n^* beginning with $(1/n^*)^3$.[22] The successive powers of $1/n^{*2}$ reflect the energy dependence of the val-

TABLE II. Fine-structure intervals and polarizabilities of K d states.

n	S_d (MHz)	α_2 meas [MHz/(V/cm)^2]	α_2 calc [MHz/(V/cm)^2]	γ [MHz/(V/cm)^4]	α_0 calc [MHz/(V/cm)^2]
15	−375.33(40)	−0.0208(9)	−0.0201	$2.3\ (36)\times10^{-8}$	0.100
16	−306.25(15)	−0.0315(8)	−0.0312	$3.32(37)\times10^{-7}$	0.156
18	−211.68(20)	−0.0681(18)	−0.0699	$2.45(20)\times10^{-6}$	0.351
20	−152.42(45)	−0.1349(40)		$1.62(23)\times10^{-5}$	

TABLE III. Parameters for fs expansions.

	A (GHz)	B (GHz)	C (GHz)
Na [a]	−96.5	498.5	...
K	−1134.3(5)	−14410(70)	72470(2300)
Rb [b]	10800(15)	−84870(100)	...

[a] See Ref. 2.
[b] See Ref. 4.

ence electron's wave function at the ionic core. The fs intervals of Na and Rb can be fitted by only two terms. For K, however, a $(1/n^*)^7$ term must be added to produce a reasonable fit to the data for n down to 4 (even the inclusion of this term does not allow us to fit $n=3$). Using the K fs intervals compiled by Moore,[23] for $n \geq 4$ we are able to fit the K fs intervals by

$$S_d = \frac{A}{(n^*)^3} + \frac{B}{(n^*)^5} + \frac{C}{(n^*)^7} \quad . \tag{8}$$

We determined the value of A solely from the $n = 15-20$ data, ignoring the $(1/n^*)^7$ term and determined B and C by fitting all the fs intervals but $n=7$ and 8 to Eq. (8) holding A fixed. We have omitted the fs intervals for $n=7$ and 8 because they are clearly inaccurate, as shown by Fig. 9.

In Table III we give values of A, B, and C for Na, K, and Rb. We show the measured and fitted [from Eq. (8)] values of $S_d(n^*)^3$. Note that even with the inclusion of the $C/(n^*)^7$ term the $n=3$ fs does not fall on the curve. We should point out that a plot of the Na and Rb fs intervals would appear as a line on a graph such as Fig. 9.

Since K has eight more electrons than Na, it is not at first surprising that the first two terms of Eq. (8). However, it is surprising that for Rb, which has 18 more electrons than K, the d fs intervals can be represented with only the first two terms of Eq. (8). Thus, it is clearly not the total number of electrons that is important.

ACKNOWLEDGMENTS

This work was supported directly by NSF Grant No. PHY76-24541 and benefitted from the use of a laboratory computer furnished under NSF Grant No. PHY76-14436. We are indebted to M. L. Zimmerman and D. L. Huestis for computer programs used to calculate radial matrix elements and to do curve fitting. We would like to thank R. M. Sternheimer for useful suggestions and encouragement. We would like to thank W. Wong, W. Wadsworth, and D. D. Lee for the generous loan of the radio-frequency signal generators and the frequency counter.

[1] W. E. Cooke, T. F. Gallagher, R. M. Hill, and S. A. Edelstein, Phys. Rev. A 16, 1141 (1977).
[2] C. M. Fabre, M. Gross, and S. Haroche, Opt. Commun. 13, 393 (1975).
[3] Y. Kato and B. P. Stoicheff, J. Opt. Soc. Am. 66, 490 (1976).
[4] K. C. Harvey and B. P. Stoicheff, Phys. Rev. Lett. 38, 537 (1976).
[5] L. Holmgren, I. Lindgren, J. Morrison, and J. M. Martensson, Z. Phys. A 276, 179 (1976).
[6] E. Luc-Koenig, Phys. Rev. A 13, 2114 (1976).
[7] H. M. Foley and R. M. Sternheimer, Phys. Lett. A 55, 276 (1975).
[8] T. Lee, J. E. Rodgers, T. D. Das, and R. M. Sternheimer, Phys. Rev. A 14, 51 (1976).
[9] T. F. Gallagher, L. M. Humphrey, R. M. Hill, W. E. Cooke, and S. A. Edelstein, Phys. Rev. A 15, 1937 (1977).
[10] A. Khadjavi, A. Lurio, and W. Happer, Phys. Rev. 167, 128 (1968).
[11] H. Kopferman, *Nuclear Moments* (Academic, New York, 1958).
[12] K. C. Harvey, R. T. Hawkins, G. Meisel, and A. L. Schawlow, Phys. Rev. Lett. 34, 366 (1974).
[13] R. T. Hawkins, W. T. Hill, F. V. Kowalski, A. L. Schawlow, and S. Svanberg, Phys. Rev. A 15, 967 (1977).
[14] T. F. Gallagher, L. M. Humphrey, R. M. Hill, and S. A. Edelstein, Phys. Rev. Lett. 37, 1465 (1976).
[15] T. F. Gallagher and W. E. Cooke (unpublished).
[16] H. K. Hughes, Phys. Rev. 72, 614 (1947).
[17] R. F. Stebbings, C. J. Latimer, W. P. West, F. B. Dunning, and T. B. Cook, Phys. Rev. A 12, 1453 (1975).
[18] T. W. Ducas, M. G. Littman, R. R. Freeman, and D. Kleppner, Phys. Rev. Lett. 35, 366 (1975).
[19] A. D. Buckingham, *Advances in Chemical Physics* (Interscience, New York, 1967), Vol. 12, p. 107.
[20] D. R. Bates and A. Damgaard, Philos. Trans. Soc. Lond. 242, 101 (1949).
[21] M. L. Zimmerman (private communication).
[22] K. B. MacAdam and W. H. Wing, Phys. Rev. A 12, 1465 (1975).
[23] C. E. Moore, *Atomic Energy Levels*, Natl. Bur. Stand. (U.S.) Circ. No. 467 (U.S. GPO, Washington, D. C., 1949).